Towards 10^{10} Contrast for NASA's Terrestrial Planet Finder Mission: Demonstration of High Contrast in a Shaped-Pupil Coronagraph at Princeton

Ruslan Belikov[1]†, James Beall[2], Michael Carr[1], Amir Give'on[1], Jason Kay[1], Taofik Kolade[1], Michael Littman[1], Frank Mycroft[1], Laurent Pueyo[1], Robert J. Vanderbei[1], and N. Jeremy Kasdin[1]

[1]Princeton University, Princeton, NJ
[2]National Institute of Standards and Technology, Boulder, CO

Abstract. Our group at Princeton University is developing the Shaped-Pupil Coronagraph (SPC) as a solution to the high contrast imaging requirements for NASA's Terrestrial Planet Finder mission. At the heart of the SPC is a specially designed shaped mask at the pupil plane, and a star occulter at the image plane. We report a measurement of 10^5 contrast at 4 λ/D and 10^6 at 7 λ/D, with no adaptive optics corrections. This contrast is maintained at laser wavelengths of 532, 594, and 632nm, and for broadband light from at least 550nm to 750nm. The contrast is almost certainly limited by wavefront aberrations in the mirrors. Indeed, the level and general structure of the speckles in the high contrast region is consistent with statistical simulations of our optics.

Keywords. space vehicles: instruments, methods: laboratory, planets and satellites: general, stars: planetary systems, instrumentation: high angular resolution, instrumentation: adaptive optics, astrobiology, extraterrestrial intelligence.

---

1. Introduction

NASA's Terrestrial Planet Finder Coronagraph (TPF-C) is expected to be the first instrument to directly image and characterize an Earth-like extrasolar planet, sometime in the next decade. It will consist of a space telescope with a high-contrast imaging system required to have 10^{10} contrast at inner working angles of 4 λ/D in visible wavelengths for the TPF-C 8x3.5m primary. Many groups are prototyping extreme coronagraph concepts with the goal of demonstrating high contrast in the lab (see, for example, Trauger 2005, Chakraborty 2004, Crepp 2005, Wilhelmsen 2004). Most notably, the group at the Jet Propulsion Laboratory (JPL, Trauger 2005) have demonstrated a contrast level of 10^9 in monochromatic light with a variant of the conventional Lyot coronagraph and an adaptive optics (AO) wavefront control system in a vacuum chamber. Over the past 5 years, our group at Princeton University has been pioneering the Shaped-Pupil Coronagraph (SPC) as an alternative to the more traditional methods. We favor the SPC because it is very simple to manufacture, is inherently broadband, and has minimal sensitivity to aberrations and off-axis effects (Green 2004), while maintaining competitive performance with respect to other approaches. More details can be found in our recent paper (Kasdin

† Present address: Princeton University, MAE Dept., Olden St, Princeton, NJ08544
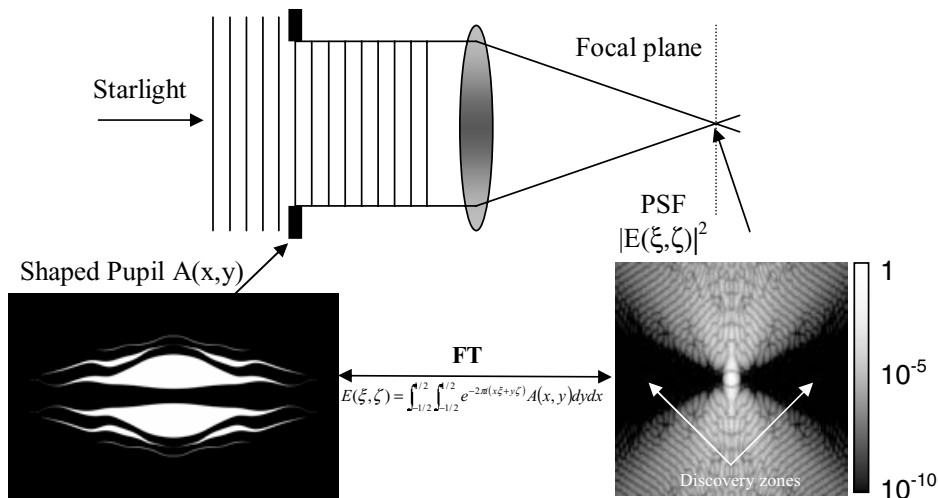email: rbelikov@princeton.edu

Figure 1. The Shaped Pupil Coronagraph concept. Shown are our chosen shaped pupil design (nicknamed "ripple") and the corresponding PSF.

2005), which contains a general overview of the design, manufacturing, and experimental results.

In this paper, we focus on our laboratory efforts and results. In section 2, we give a brief overview of the shaped pupil concept and describe our lab and the optical setup. In section 3, we describe our results to date, most notably the demonstration of 10^5 contrast at 4 λ/D, which gradually drops to 10^6 level at 7 λ/D, and continues dropping as working angle is increased. It should be noted that these results were achieved in the absence of any wavefront control system.

2. Laboratory Setup

At the heart of the SPC is an appropriately shaped mask at the pupil plane, as shown in Figure 1. With a shaped pupil in place, the point spread function (PSF) of the idealized system is no longer an airy pattern, but the Fourier Transform of the shaped pupil. (More precisely, the PSF is the magnitude squared of the Fourier transform of the indicator function of the shaped pupil). One can design this shaped pupil to yield a concentrated PSF which has high contrast regions, or discovery zones, where a dim planet can be found (Kasdin 2003). After some design effort (Vanderbei 2003), we converged on our currently favorite design shown in Figure 1, nicknamed "ripple", based on what we think is a good tradeoff between throughput and extent of the discovery zone, as well as the simplicity of manufacture. The PSF corresponding to the ripple design has the required 10^{10} contrast ratio within 2 discovery zones, each having a 45 degree opening and a working angle range of 4 to 100 λ/D, where D is the long axis of the ripple mask. The Airy throughput is 30%. (Throughout this paper, by "contrast" we mean the ratio of the peak PSF intensity to the discovery zone intensity, and use the term "suppression" to mean the inverse of contrast. "Airy throughput" is the energy that falls into the main lobe of the PSF measured relative to the total energy conveyed through a fully open aperture.) We have manufactured a mask based on the ripple design at the National Institute of Standards and Technology in Boulder, CO, out of a 76mm diameter double-side polished silicon wafer (Kasdin 2005).
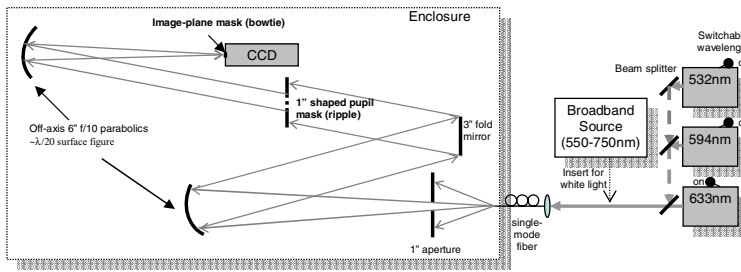
Figure 2. Laboratory setup.

Our lab consists of a 1.2x5m vibration-isolated optical bench with an enclosure to eliminate thermal convection, particulate contamination, and stray light. We also use HEPA filters to further reduce particulate contamination and an AC system to stabilize the temperature and humidity. The optical bench setup is shown in Figure 2. It is meant to recreate the simple schematic of Figure 1 with the goal of imaging the PSF of the shaped pupil and measuring the contrast in the discovery zones. Several sources were set up as inputs to our system: a 5mW doubled YAG laser pointer head at 532nm; 2 He-Ne lasers at 594nm (2mW), and 632nm (5mW) respectively; and a Tungsten lamp white light source with color temperature of 3200K. These sources are coupled into a single mode fiber which enters the enclosure. In the enclosure the fiber serves as a point light source to simulate a star. The diverging Gaussian beam from the fiber first goes through a 1" aperture, gets collimated by a 6" off-axis parabola, redirected by a 3" flat fold mirror, and finally illuminates the shaped pupil. The collimated beam is now 3" in diameter (which is determined by the 1" aperture and is matched to the 3" fold mirror). The beam illuminating the shaped pupil has approximately a flat wavefront and a uniform amplitude profile, especially over the 1" area of the shaped pupil. The beam goes through the shaped pupil, and is focused onto a cooled CCD by a second off-axis parabola. The CCD then records the PSF, as shown in Figure 3a, with exposures typically lasting 1 second. Due to the high 10^{10} dynamic range of the PSF, the bright core of the PSF will overwhelm the CCD circuitry and scatter inside the camera, creating undesirable artifacts in the discovery zones. To avoid these artifacts, we manufactured an image plane mask to block all of the PSF except for the discovery zones. This mask, which we call "bowtie", sits 1-2mm away from the sensitive area of the CCD chip, which is still essentially at focus. A simulation of the portion of the PSF blocked by the bowtie is shown in Figure 3b.

Since we cannot measure the intensity of the core with the bowtie in place, we have to estimate the PSF core intensity some other way in order to properly calibrate the contrast measurements. There are two methods for doing this. In the first, direct method, we take an unsaturated exposure of the PSF core (no bowtie, low power and short integration time), and use that measurement to extrapolate the intensity of the PSF core in full power exposures, where the core is blocked by the bowtie. An alternative, easier method uses the portions of the PSF beyond the outer working angle (OWA) of 100 λ/D instead of the main core. This "OWA structure", shown in 3a and b, corresponds to the portion of the ideal PSF beyond the discovery zone, and thus has a known shape and contrast (which peaks at about 10^6). Note the good correspondence of the theoretical and experimental OWA structures in Figure 3b. Measurements of the dark zone contrast can thus be directly obtained by using the OWA structure as a reference, as long as it is not saturated.
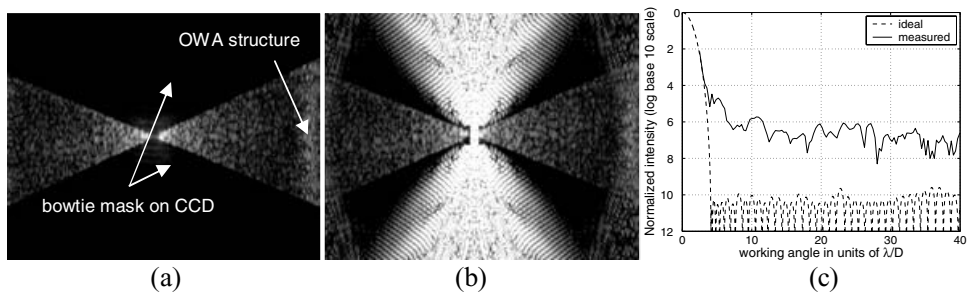
Figure 3. (a) Logarithmically stretched CCD image of the discovery zones, at 632nm, showing a region from roughly -100 λ/D to 120 λ/D (b) Same as (a), but with a superimposed simulation of what the bowtie is blocking. (c) A horizontal slice through the image in (a) from 0 to 40 λ/D.

3. Results

As can be seen in Figure 3, the measured discovery zones contain a lot of speckle. A horizontal slice through the center of the image is shown in Figure 3c. The suppression (inverse of contrast) is about 3×10^{-5} at 4 λ/D, gradually dropping to slightly higher than 10^{-6} after 7 λ/D. (By 100 λ/D, it is down to almost 10^{-8}). These values can change if the mask is laterally shifted, because in that case slightly different areas of the mirrors with different aberrations are effectively being used. There are some positions of the shaped pupil where the suppression drops to 10^{-5} at $4\lambda/D$, for example, but at the expense of worsening the contrast at 7 λ/D.

To determine whether aberrations in the optics are indeed the dominant cause of the speckle in our images, we conducted a series of tests. First, we noted that the speckle pattern is quite stable. Exposures taken seconds apart agree to at least 1 part in 100, and exposures taken an hour apart agree to about 1 part in 10. (And this discrepancy may simply be due to a technical issue such as an instability in laser power). Furthermore, the speckle pattern remains qualitatively the same over days or even weeks until the setup is perturbed somehow. Thus, aberrations due to air or mechanical instabilities are not dominant. We then looked at the effects of transversely shifting the shaped pupil. When it is shifted by as little as 1mm, the entire speckle pattern changes. As mentioned above, what we are really varying by transversely shifting the shaped pupil is the region of the mirrors being used. Since all the speckles change, they must be due to the mirror aberrations. The only part of the image that does not change is the OWA structure, because it in fact is a function of the shaped pupil itself and not the mirror aberrations.

Finally, we conducted a simple statistical simulation of the speckle for our optics, based on their peak-to-valley surface figure rating of $\lambda/20$. The simulation consisted of the following steps: (1) create a random phase variation across the plane of the shaped pupil with power spectral density of $1/f^{\alpha}$, where α is a free parameter to be fitted; (2) scale this phase error to correspond to the combined surface figure of the 3 mirrors; (3) multiply by the shaped pupil; (4) Fourier Transform. The results are shown in Figure 4. Qualitatively, the speckle pattern in the simulation looks about the same as in the measurements, and quantitatively, on the graph, the general level of the simulated speckle seems to match the measured speckle, at least to the extent that two random processes can match. We conclude that our contrast is dominated by wavefront error of the optics, which requires adaptive optics for correction.

So far, the data we have shown has been at 632nm. In Figure 5, we show the images and contrast measurements at 3 different wavelengths. It is apparent from Figure 5 that the PSF dilates with wavelength, as it must. The graph on the right of Figure 5
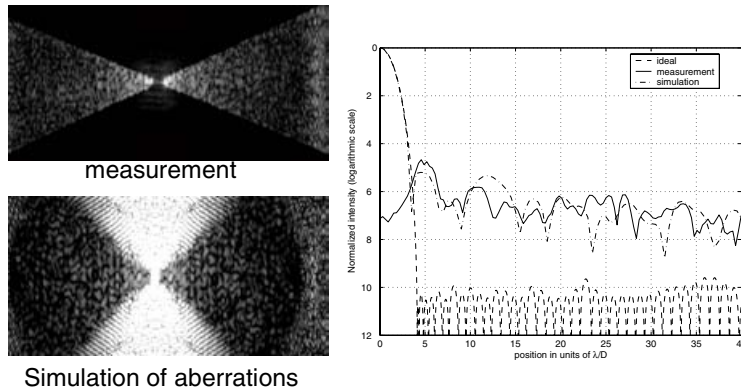
Figure 4. Simulation of random phase aberrations (phase only) based on the quality of our mirrors.
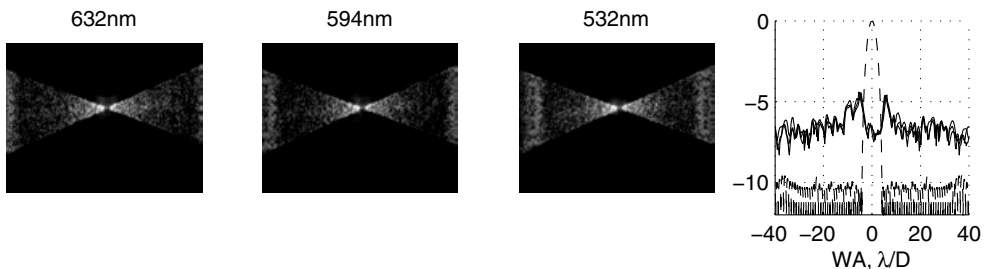

Figure 5. Measurements at 3 different wavelengths. Right: superimposed slices for the three measurements (dashed line is the ideal PSF).

shows superimposed horizontal slices through the centers of the 3 images, going out to 40 λ/D. These traces have been stretched along the abscissa to reverse the dilation due to wavelength, so that all are plotted on the same λ/D scale. Two things on this graph are noteworthy. First, the contrast is the same for different wavelengths, showing the broadband capability of shaped pupils. Second, the speckle structure itself looks very similar for different wavelengths, especially for the lower working angles. However, they are not completely identical. We expect the speckle to be slightly higher at shorter wavelengths because the phase aberrations are effectively greater, but such a difference is almost imperceptible across a scale of 12 orders of magnitude and cannot account for the variations apparent in the plot. There are many reasons why the traces can exhibit these differences, such as: wavelength-dependent amplitude aberrations, higher order speckle effects such as frequency folding, different behavior in the fiber, etc. Tracking down the exact reasons will be important for understanding how to correct them.

In Figure 6, we present the results of our measurements in broadband light. The spectrum of our light source is shown in Figure 6b, and goes from approximately 550nm to 750nm. The speckle image appears rather noisy because the white light power is very low, due to the inherent inefficiencies in coupling a spatially incoherent light source into a single mode fiber. Because of this, electronic noise limits the measurements of speckle level to about $4\text{x}10^{-7}$. Nonetheless, it is still clear from Figure 6c that the contrast in broadband light remains the same as in monochromatic light and that even the speckle structure is very similar, at least for low inner working angles. This once again shows the broadband capabilities of shaped pupils.
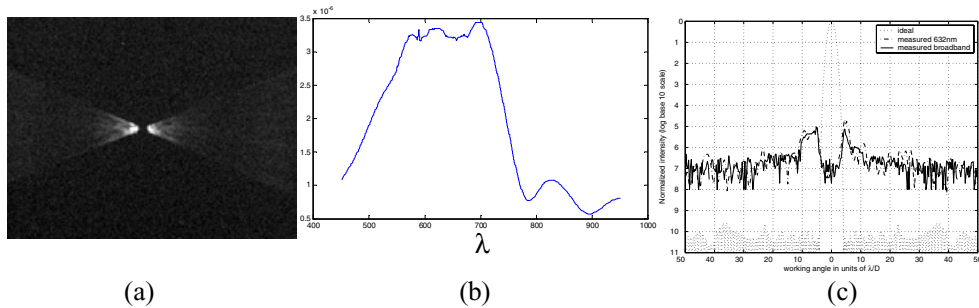
Figure 6. (a) CCD image in white light (1 hour exposure); (b) Measured spectrum before the fiber; c Slice through the CCD image.

4. Final Remarks

We have demonstrated high contrast in a prototype Shaped-Pupil Coronagraph, which is currently limited by aberrations in the optics. This contrast is maintained over different wavelengths and over broadband light. However, it is still far from the designed 10^{10} value. In order for the full 10^{10} contrast to be reached, aberrations need to be corrected by adaptive optics. It is believed that correction to $\lambda/10^5$ rms level would be required. Furthermore, amplitude aberrations and wavelength dependency of aberrations cannot be neglected. Work in several groups, including ours, is energetically proceeding on this problem (see, for example, Pueyo 2004, Borde 2005, Give'on 2005, and Redding 2002).

Acknowledgements

References

Borde P. & Traub W., *astro-ph/0511326*, 2005

Chakraborty, A. & Thompson, L. A., *Optics Express* Vol. 13, No. 7, pp. 2394-2402, 2004

Crepp, J., Ge, J., Debes, J., Kuchner, M., & McDavitt, D., *Proc. of SPIE* 5487 (1383C), 2005

Give'on, A., Kasdin, N. J., & Vanderbei, R. J., *Proceedings of IAUC 200*, 2005

Green, J. J., Shaklan, S. B., Vanderbei R. J., & Kasdin, N. J., *Proc. of SPIE* 5487(184), 2004

Kasdin, N. J., Vanderbei, R. J., Spergel, D. N., & Littman, M. G., *The Astrophysical Journal* 582, pp1147-1161, January 2003

Kasdin, N. J., Belikov, R., Beall, J., Vanderbei, R. J., Littman, M. G., Carr, M., & Give'on, A. *Proc. of SPIE* Vol. 5905, pp. 0G1-0G9, 2005

Pueyo, L., Give'on, A., Carr, M., Littman, M., Kasdin, N. J., & Vanderbei, R. J., *Proc. of SPIE*, 5487(184), 2004

Redding, D., Green, J., Basinger, S., Cohen, D., Dumont, P., Hull, T., Moody, D., Trauger, J., Shaklan S., & Shi, F., *Proc. of SPIE*, 4854(40), 2002

Trauger, J., Brown, M., Brown, R. A., Burrows, A., Burrows, C., Ealey, M., Fischer, D., Ftaclas, C., Heap, S., Hull, T., Kasdin, J., Krist, J., Kuchner, M., Lunine, J., Marcy, G., Sahai, R., Spergel, D., Stapelfeldt, K., Traub, W., & Woodgate, B. *Proc. of AAS, DPS meeting 37*, 18.24, 2005

Vanderbei, R. J., Spergel, D. N., Kasdin, N. J., & Kuchner M., *Proc. of SPIE*, 5170(49), 2003

Wilhelmsen, Evans, J., Sommargren, G., Poyneer, L., Macintosh, B. A., Severson, S., Dillon, D., Sheinis, A. I., Palmer, D., Kasdin, N. J., & Olivier, S., *Proc. of SPIE* 5490(954), 2004